Supporting information

Journal of Material Chemistry A

Graphene supported pyrene functionalized amino-carbon nanotube: a novel hybrid architecture of Laccase immobilization as effective bioelectrocatalyst for oxygen reduction reaction

Aso Navaee [a] , Abdollah Salimi [a,b]*

a-Department of Chemistry, University of Kurdistan, , 66177-15175, Sanandaj- Iran

Research Centre for Nanotechnology, University of Kurdistan, 66177-15175, Sanandaj- Iran,

e-mail:absalimi@uok.ac.ir

Preparation of graphene oxide (GO) and graphene (Gr): We synthesized Gr using modified hummers method as described in our previous work.[S1] In brief; 1 g graphite powder was added to 3 g of $NaNO_3$ and 25 ml of concentrated H_2SO_4 in an ice bath. Then, 3 g $KMnO_4$ was gradually added at 15 min under stirring. The mixture was stirred for 2 h at ambient temperature and then diluted with DI water and stirred for 30 min. After that, 5% H_2O_2 was added into the solution until the color of the mixture changed to yellow, indicating that graphite is fully oxidized. The as-obtained graphite oxide slurry was re-dispersed in DI water and then exfoliated to generate graphene oxide nanosheets using a bath ultrasonic. The mixture was then filtered and washed with diluted HCl solution to remove metal ions. Finally, the product was washed with DI water to remove the acid. Afterwards, the graphene oxide nanosheets have been reduced by hydrazine. In a typical process, 50 mg of obtained solid product were redispersed in 20 ml of H_2O via ultrasonication. Then 100 mg poly (sodium 4-styrenesulfonate) (PSS, $(C_8H_7NaOS)_n$, Mw = 70,000) and 2.5 ml hydrazine (NH_2NH_2) were added into the GO dispersion. After stirring for 30 min, the mixture was transferred to a Teflon lined autoclave and held in an oven at 110 °C for 1 h. During the hydrothermal reaction, graphene oxide reacted with PSS and was simultaneously reduced by hydrazine to graphene nanosheet-PSS (GNSs-PSS). The product was centrifuged and then washed

with DI water and ethanol to remove the unreacted PSS surfactant. The final product was dried in a vacuum oven at 60 °C.

Table S1: The onset potential and current density for ORR at different LC-based modified electrodes

Electrode material	Onset potential/ V, vs. Ag/AgCl	Current density (mA cm^{-2})	Ref.
C.[a] unicolor LC/CNP in sol–gel silicate film on ITO	0.575 at pH 4.8	0.095 at 0.0 V	S2
C. unicolor LC/ Anthracene modified SWCNT	0.612 at pH 5.2	0.246 at 0.2 V	S3
C. unicolor LC/pyrene/vertically aligned CNT	0.600 at pH 4.8	0.400 at 0.4 V	S4
T.[b] hirsuta LC/Au NP/Au	0.65 at pH 4	0.01 at 0.2 V	S5
T. hirsuta LC/phenol derivatives/ graphite	0.60 at pH 5.1	0.5 at 0.2 V	S6
T. hirsuta Laccase covalently on Au	0.65 at pH 4.2	0.04 at 0.2 V	S7
T. versicolor LC/ Anthracene-2-methanethiol-Au	0.91 at pH 4.0	0.025 at 0.23 V	S8
T. versicolor LC/Anthracene -MWCNTs	0.62 at pH 4.5	0.14 at 0.2 V	S9
Cerrena maxima LC/carbon nanoparticles	0.74 at pH 5.5	0.044 at 0.0 V	S10
T. versicolor LC/MWCNT/Polypyrrole-pyrene/LC	0.6 at pH 5.0	1.85 at 0.0 under O_2 purging	S11
T. versicolor LC/MWCNT/pyr-$(AQ)_2$[c]	0.61at pH 5	0.8 at 0.2 V	S12
T. hirsuta LC/anthraquinone-3D-CNT	0.5 at pH 5	0.4 at 0.2 V	S13
T. hirsuta LC/nanoporous Au	0.65 at pH 4.0	0.028 at 0.2 V	S14
T. versicolor LC/PBA-amino-CNTs-Gr	0.64 in pH 5	0.8 at 0.3 V	This work

[a] Cerena, [b] Trametes, [c] 1-[bis(2-anthraquinonyl)aminomethyl]-pyrene

Koutecky–Levich plots: The current signals were analyzed in accordance to the Koutecky–Levich plots. Extrapolating to the intersection with the y-axis, when $\omega \rightarrow \infty$ and $1/J \rightarrow 0$, the limit current can be found form the enzyme kinetics. For the proposed modified electrode the obtained J_{cat} value was 1.92 mA cm^{-2}.

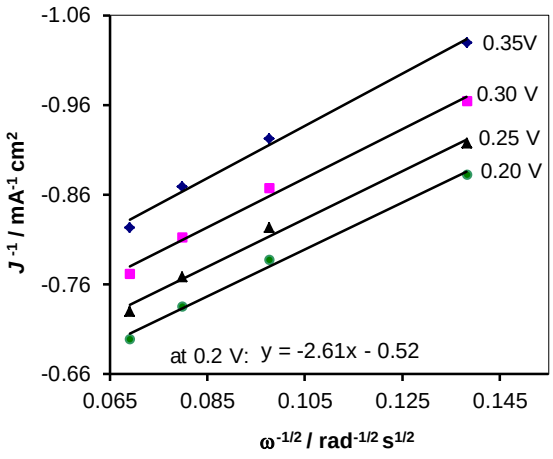

Figure S1: Koutecky-Levich plots from the RDE analysis for the LC/PBA-amino-CNT-Gr modified electrode at different points of plateau region.

Study of the pH effect and the stability of modified electrode over time: The catalytic activity of LC/amino-CNTs-Gr-based electrode was examined at three different pHs near to the physiological condition (5.0, 6.0 and 7.0). As can be seen in Figure S2, at all conditions, the modified electrode shows a superior biocatalytic activity toward ORR, but at pH=5 provides highest biocatalytic activity toward ORR which at plateau region the current density increases up to 0.8 mA cm^{-2}. By increasing the pH values up to 7.0, the current density slightly decreases to 0.33 mA cm^{-2}, indicating the highest catalytic activity of LC in slightly acidic pHs. Among them, we selected the pH=5 to study all other biocompatibility and biocatalytic activity.

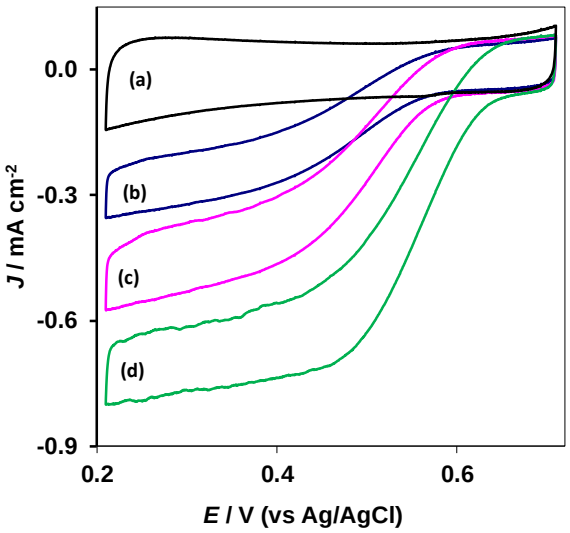

Figure S2: Recorded CVs from LC modified electrode in N_2 saturation condition (a) and O_2 saturation condition in pH=7 (b), pH=6 (c) and pH=5 (d).

The modified electrode exhibits preferable stability over time where, after 4 days from the first application, a little depletion, about 7% in the catalytic current is observed (Figure S3A). Moreover, the continuous biocatalytic activity of the modified electrode was examined using choronoamperometry technique. As shown in Figure S3B, with the passage of time the depletion in the current density is not seen over ~4 hours. This results show good stability of the LC-based electrodes.

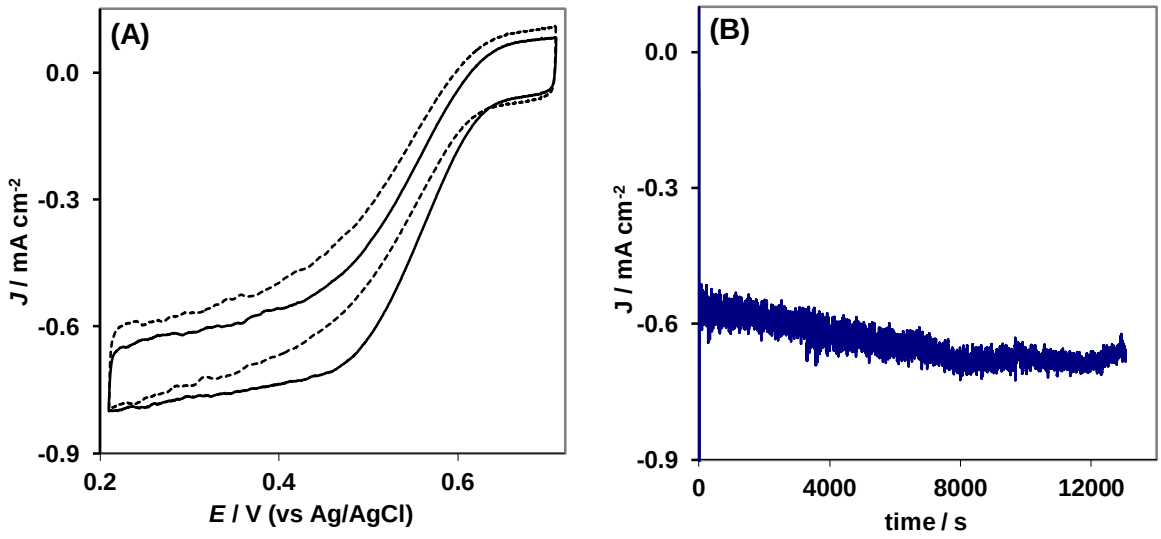

Figure S3: A) Recorded CVs of the LC/PBA-amino-CNT-Gr under O_2 saturation condition in the first application (smoothed line) and after 4 days (dotted line). B) Choronoamperogram obtained by LC/PBA-amino-CNT-Gr modified electrode under O_2 atmosphere during continues 4 hours.

References

S1 A. Navaee, A. Salimi and H. Teymourian, *Biosens. Bioelectron*. 2012, **31**, 205-211.

S2 K. Szot, W. Nogala, J. Niedziolka-Jönssona, M. Jönsson-Niedziolka, F. Marken, J. Rogalskic, C.N. Kirchner, G. Wittstock and M. Opallo, *Electrochim. Acta* 2009, **54**, 4620-4625.

S3 K. Stolarczyk, M. Sepelowska, D. Lyp, K. Zelechowska, J.F. Biernat, J. Rogalski, K.D. Farmer, K.N. Roberts and R. Bilewicz, *Bioelectrochemistry* 2011, **87**, 154-163.

S4 A. Zloczewska, M. Jönsson-Niedziolka, J. Rogalski and M. Opallo, *Electrochim. Acta* 2011, **56**, 3947-3953.

S5 M. Dagys, K. Habreska, S. Shleev, T. Arnebrant, J. Kulys and T. Ruzgas, *Electrochem. Comm*. 2010, **12**, 933-935.

S6 C. Vaz-Dominguez, S. Campuzano, O. Rüdiger, M. Pita, M. Gorbacheva, S. Shleev, V.M. Fernandez and A.L. De Lacey, *Biosens. Bioelectron.* 2008, **24**, 531-537.

S7 M. Pita, C. Gutierrez-Sanchez, D. Olea, M. Velez, C. Garcia-Diego, S. Shleev, V. M. Fernandez and A. L. De Lacey, *J. Phys. Chem. C* 2011, **115**, 13420–13428.

S8 M. S. Thorum, C. A. Anderson, J.J. Hatch, A. S. Campbell, N.M. Marshall, S.C. Zimmerman, Y. Lu and A.A. Gewirth, Direct, *J. Phys. Chem. Lett*. 2010, **1**, 2251–2254.

S9 M.T. Meredith, M. Minson, D. Hickey, K. Artyushkova, D.T. Glatzhofer and S.D. Minteer, *ACS Catal*. 2011, **1**, 1683–1690.

S10 U.B. Jensen, M. Vagin, O. Koroleva, D.S. Sutherland, F. Besenbacher, and E.E. Ferapontova, *J. Electroanal. Chem.* 2012, **667**, 11–18.

S11 N. Lalaoui, K. Elouarzaki, A. Le Goff, M. Holzinger and S. Cosnier, *Chem. Commun.* 2013, **49**, 9281-9283.

S12 M. Bourourou, K. Elouarzaki, N. Lalaoui, C. Agnes, A.L. Goff, M. Holzinger, A. Maaref and S. Cosnier, *Chem. Eur. J*. 2013, **19**, 9371-9375.

S13 M. Sosna, L. Stoica, E. Wright, J.D. Kilburn, W. Schuhmannc and P.N. Bartlett, *Phys. Chem. Chem. Phys*. 2012, **14**, 11882–11885.

S14 U. Salaj-Kosla, S. Pöller, W. Schuhmann, S. Shleev and E. Magner, *Bioelectrochemistry* 2013, **91**, 15–20.